

Online control algorithm for sub-half-hourly operation of LV-connected energy storage device owned by DNO

Conference or Workshop Item

Published Version

Creative Commons: Attribution 3.0 (CC-BY)

Open Access

Yunusov, T. ORCID: <https://orcid.org/0000-0003-2318-3009>, Zangs, M. J., Holderbaum, W., Fila, M. and Potter, B. (2018) Online control algorithm for sub-half-hourly operation of LV-connected energy storage device owned by DNO. In: CIRED 2017, 12-15 June 2017, Glasgow, UK, pp. 1342-1346. Available at <https://centaur.reading.ac.uk/69912/>

It is advisable to refer to the publisher's version if you intend to cite from the work. See [Guidance on citing](#).

Published version at: <http://doi.org/10.1049/oap-cired.2017.0481>

All outputs in CentAUR are protected by Intellectual Property Rights law, including copyright law. Copyright and IPR is retained by the creators or other copyright holders. Terms and conditions for use of this material are defined in the [End User Agreement](#).

www.reading.ac.uk/centaur

Central Archive at the University of Reading

Reading's research outputs online

Online control algorithm for sub-half-hourly operation of LV connected energy storage device owned by DNO

Timur Yunusov¹ ✉, Maximilian Zangs¹, William Holderbaum², Maciej Fila³, Ben Potter¹

¹School of Built Environment, University of Reading, Reading, UK

²Manchester Metropolitan University, Manchester, UK

³Scottish and Southern Electricity Networks, Reading, UK

✉ E-mail: t.yunusov@reading.ac.uk

Abstract: Change in consumer behaviour through uptake of low carbon technologies is likely to put existing distribution networks under strain and worsen the operational requirements of the network. Deployment of energy storage and power electronics is a feasible alternative to traditional network reinforcement. This study presents two control algorithms used with an energy storage device deployed as part of New Thames Valley Vision Project. The two algorithms are aimed at (i) equalising phase loading with correction of power factor and (ii) providing voltage support with Additive Increase Multiplicative Decrease algorithm for active and reactive power control.

1 Introduction

With the transition towards the low carbon economy and uptake of low carbon technologies (LCTs), consumers' behaviours change and could create conditions where the operational constraints on the LV network are violated. The Distribution Network Operators (DNOs) are facing the challenge of maintaining power quality and network operation (e.g. voltage and thermal constraints) while permitting integration of LCTs. The majority of domestic consumers in the UK are supplied through single-phase connections and, with the addition of single-phase LCTs, could further deteriorate power quality and increase the probability of violating operational constraints [1].

As part of the New Thames Valley Vision (NTVV) project, Scottish and Southern Energy Networks (SSEN) set out to investigate how energy storage and power electronics are deployed on existing low voltage (LV) network to support the network in transition to a low carbon economy. Together with academic partners, the NTVV project has developed tools and techniques to better understand how demand is changing and how control of energy storage could meet technical requirements for network operation. One of the developed tools is the Smart Control system. This system is designed to operate Energy Storage and Management Units (ESMUs) on the LV network to support network operation based on short-term demand forecast and data from network monitoring.

This paper presents two online control algorithms included in the Smart Control system and compares their anticipated performance with the results from field trials. The first control algorithm is designed to balance loading between phases with active power transfer while also providing power factor (PF) correction through injection of reactive power.

2 Project overview

The NTVV project aims to demonstrate that DNOs could develop more efficient networks for the low carbon economy by understanding, anticipating, and supporting the changes in consumer behaviour. Data analytics have been applied to process demand data collected from monitoring 300 LV substations and

200 end point monitors, to give a clearer understating of consumer demand and how it could change. Network modelling in combination with demand modelling have provided an insight in how to improve network operation, planning, and investment management. The outcome of this modelling process is used to advise on the techniques for supporting the networks in the light of changing consumer behaviour. One of the solutions for supporting distribution networks is deployment of energy storage and power electronics devices at the LV level. To explore the effectiveness of the network reinforcement with energy storage, SSEN have deployed 25 ESMUs in suburban distribution network located in Bracknell, county Berkshire, UK.

2.1 Energy storage and management units

ESMU is a modular unit, depicted in Fig. 1, consists of power electronics unit (PEU) and energy storage unit (ESU). PEU is a four-quadrant three-phase inverter rated at 12 kVA per phase. Each ESU contains Battery Management System and lithium-ion battery modules with a total capacity of 12.5 kWh per module. In addition to the internal telemetry data, ESMUs also measure phase-to-phase and phase-to-neutral voltages at the point of connection.

The aim of the ESMUs within the NTVV is to evaluate their effectiveness to improve network operation, as shown in Table 1, and aid in the assessment for alternative network reinforcement methods.

The majority of customers' connections in the UK are single phase resulting in an often unbalanced loading on the feeder. Phase-balancing operation of the ESMU is aimed at equalising loading between phases by means of using power electronics to shift load between phases. The expected benefit would be lower thermal loading on the phases and neutral cables.

Typical consumer behaviour and working patterns cause a significantly higher demand during the evening hours. Consequently, the thermal constraints are also likely to be violated during those peak hours. The resulting stress on the network can be alleviated by shifting the demand from peak hours to non-peak hours. Charging the energy storage device during non-peak hours and discharging it during peak hours would provide the desired relief on the network. Lowering peak demand also improves thermal constraints and reduces network losses.



Fig. 1 ESMU with one PEU (on the right) and two ESUs (on the left) installed on a grass verge near a footpath in residential area in Bracknell, UK

Combining phase balancing and peak reduction functions would further improve the impact on the network, although the required ESMU energy storage capacity is potentially lowered. For instance, equalising loading between phases would reduce the peak demand on the most loaded phase. This consequently reduces the amount of energy required to be discharged from storage to achieve the same net peak reduction.

To maximise such benefits from ESMU operation, the units were connected to the LV feeders between half-way and two-thirds down the length of the feeder – as depicted in Fig. 2. Such placement provides similar improvement on the thermal constraints as an ESMU at the top of the feeder or substation but with additional benefit of improvement on voltage constraints [3].

The two control algorithms presented in this paper are online phase balancing and online voltage support, focusing on thermal and voltage constraints, respectively.

3 Online control

Extensive monitoring of LV substations has provided an insight on variability of demand on LV feeders at a 5 s resolution. Fig. 3 provides an example of power consumption per phase over period of 1 h.

Several Smart Control algorithms were developed for automated control of the ESMUs and were integrated with the existing distribution management system through the Active Device Distribution Management (ADDM) platform. The architecture of ADDM allows centralised management of Smart Control algorithms and conveniently provides access to the SCADA interface for delivering instructions to the ESMUs and returning data from the network monitoring. However, this centralised architecture and remote execution of instructions introduces latency between receiving measurements and generating control instruction. This means that the Smart Control algorithms cannot operation in true real time and relies on an approximation of expected network operation status.

Owing to volatility of power demand at 5 s resolution – highest available resolution for ADDM platform – it is difficult to predict demand and network status accurately at the same resolution. An approximation approach was taken where previously measured values were averaged over a period of time (e.g. 3 min) and assumed to remain constant for the next period of time of same duration – as depicted in Fig. 4.

Table 1 Anticipated impact of ESMU operation under Smart Control algorithms on the network operational requirements. ‘H’ indicates direct improvement and ‘M’ indicates where indirect improvement is likely [2]

	Voltage regulation	Voltage balance	Phase thermal	Neutral thermal	Utilisation	Losses
phase load balancing	M	M	H	H	M	M
peak spreading	M	M	H	H	H	H
voltage support	H	M				

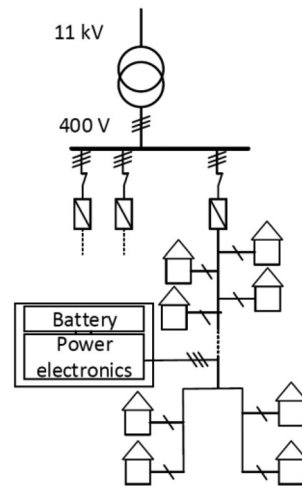


Fig. 2 Diagram of a typical ESMU location on an LV feeder

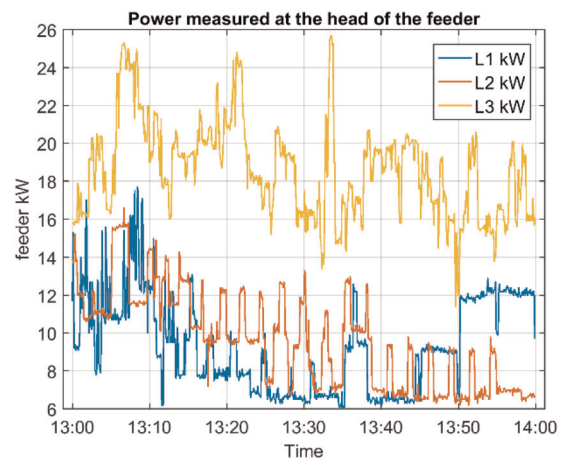


Fig. 3 Example of demand variability at 5 s resolution on an LV feeder

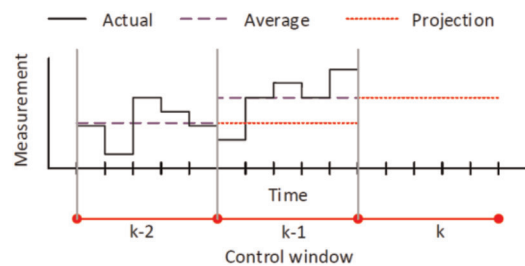


Fig. 4 Approximation of measurements through projection of average

3.1 Phase-balancing and PF correction

The phase-balancing algorithm is based on transferring power between phases to match the average power flow across to phases. Active power instruction, p^p , for each phase is given as a

difference between average phase loading, d^a , and loading on the corresponding phase, d^p , i.e. $p^p = d^a, d^p$.

If the calculated instruction value is greater than the phase KVA rating of the PEU, then the instruction value is capped to a maximum of 12 kW and the two remaining uncapped instructions are adjusted accordingly to maintain zero net power flow:

$$p^{p \notin \{p^{\text{capped}}\}} = \left| p^{p \in \{p^{\text{capped}}\}} \right| - \frac{\sum_i^3 p^i}{3 - \text{numel}(\text{uncapped})}$$

The reactive power instructions are equivalent to the negative to the projection of the reactive power flow, as measured at the source of the feeder. Here, the aim is to maintain unity PF as measured at the substation level, while operating within kVA rating of the ESMU.

3.2 Voltage support

The voltage support algorithm is based on the Additive Increase Multiplicative Decrease (AIMD) algorithm presented in [4] with addition of reactive power control. The algorithm compares the projected phase-to-neutral voltage measurement with a target voltage, V^t , with hysteresis value, h , giving upper voltage target, V^{uh} , and lower voltage target, V^{lh} :

$$V^{\text{uh}} = V^t \left(1 + \frac{h}{2} \right), \quad V^{\text{lh}} = V^t \left(1 - \frac{h}{2} \right), \quad h \in [0, 1]$$

The voltage trigger points (depicted in Fig. 5) are used to determine the required kW and kVAr instructions based on the decision trees in Fig. 6 and the following key parameters:

α is the additive coefficient for increment step k ; β the multiplicative decrease coefficient for reducing the magnitude of the instruction; ζ the ratio for increment step defined as function of measure voltage and envelop around target voltage:

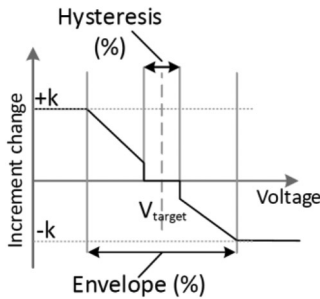


Fig. 5 Voltage trigger points for increment of injected and absorbed power for AIMD voltage support algorithm

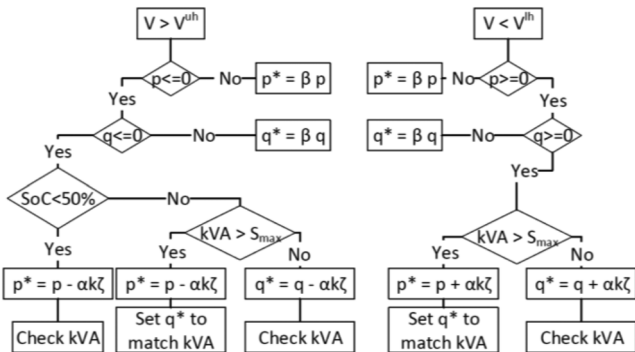


Fig. 6 AIMD decision tree for (left) high voltage events V^{uh} , and (right) LV events V^{lh}

For high-voltage events

$$\zeta = \frac{V - V^t}{V^t(1 + (e/2))}$$

For low-voltage events

$$\zeta = \frac{V - V^t}{V^t(1 - (e/2))}$$

Here, e is the envelope around the target voltage, V^t , within which the algorithm will aim to maintain phase-to-neutral voltages on all phases.

The algorithm will try to use reactive power to support voltage until the power electronics are at the maximum kVA rating. At this point, the algorithm will calculate new kW value and decrease the kVAr value to not exceed the maximum kVA rating. The only exception is for the high-voltage events when the state-of-charge (SoC) of the battery is $< 50\%$; in this case, the algorithm will prioritise on active power instructions with an aim to increase SoC. SoC also acts as a hard constraint, at 10 and 100% SoC. At those levels, the algorithm stops injecting and absorbing active power, respectively.

4 Results

Two control algorithms are simulated on an OpenDSS model of an LV feeder in Bracknell distribution network. Each load in the network was populated using synthesised demand profiled at 1 min resolution based on the CREST demand model [5] with assumed 0.95 PF. The ESMU's location in the simulation model corresponds to the actual location of the ESMU on the real feeder. For clarity, simulated results are shown for evening peak demand only – 18:45 to 19:45.

Field trial results are based on a single trial of each algorithm. Unlike simulation, the effect of the algorithms cannot be compared with a case study without ESMU operation. Instead, the data from the trials is compared with historical data for the same day of the week and time from the four previous weeks.

4.1 Phase-balancing simulation

Fig. 7 compares the active power flow per phase in the baseline case study against the case study with an operational ESMU and the corresponding line utilisation. The lower subplot in Fig. 7 shows the line utilisation for each phase. The peak demand on Phase 2 is reduced by 12 kW by shifting the load to Phases 1 and 3 (Fig. 8).

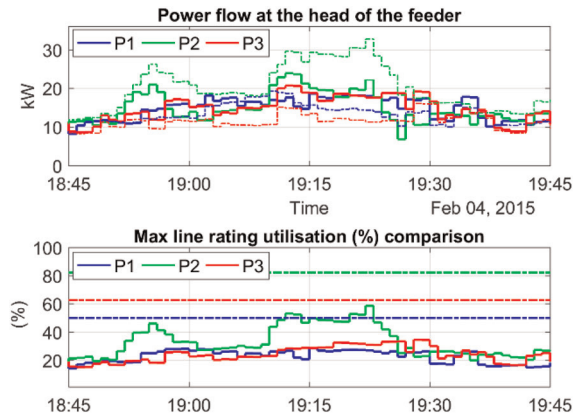


Fig. 7 (Top) Active power measures at the head of the feeder per phase: (continuous line) with ESMU, (dashed line) baseline; (bottom) line utilisation per phase: (dashed line) ESMU, (dashed dot line) maximum line utilisation in baseline study

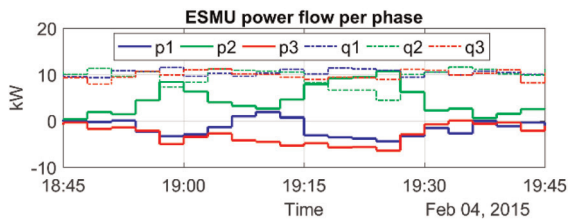


Fig. 8 Active and reactive instructions per phase for ESMU performing phase balancing and PF correction during evening peak demand. Positive values indicate power injected into the network

Table 2 PF comparison for all phases across the simulated day with ESMU performing phase balancing and PF correction

	Min	Mean	Max
baseline	0.7133	0.7289	0.7525
with ESMU	-0.2610	0.9027	1.000

This also significantly reduces the maximum line utilisation compared with baseline case study. Furthermore, PF mean power factor has also improved from 0.72 to 0.9 (Table 2).

4.2 Voltage support simulation

In Fig. 9, further deviation of Phase 2 from the lower voltage band at around 18:50 causes the AIMD algorithm to increase kW injection. At 19:10, instructions on Phase 2 reach maximum kVA rating, which lead to reduction in kVAR to allow further injection of kW (as shown in Fig. 10). In response to increase in voltage on Phase 2 at 19:15, AIMD algorithm decreased the kVAR injection on Phase 2.

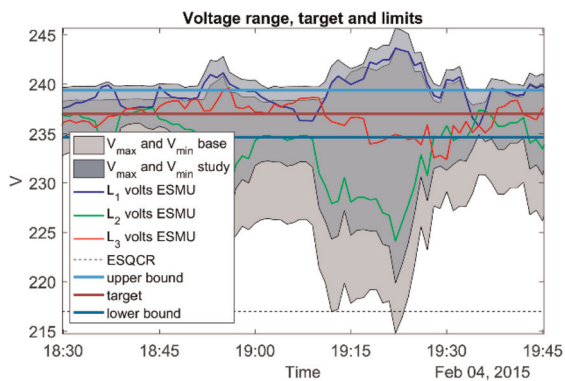


Fig. 9 Comparison of phase-to-neutral voltage range on the feeder for baseline and with AIMD

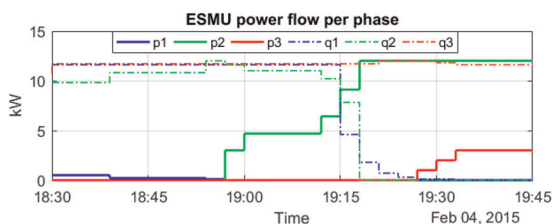


Fig. 10 ESMU reactive (dashed line) and active power (continuous line) injection per phase under AIMD voltage support

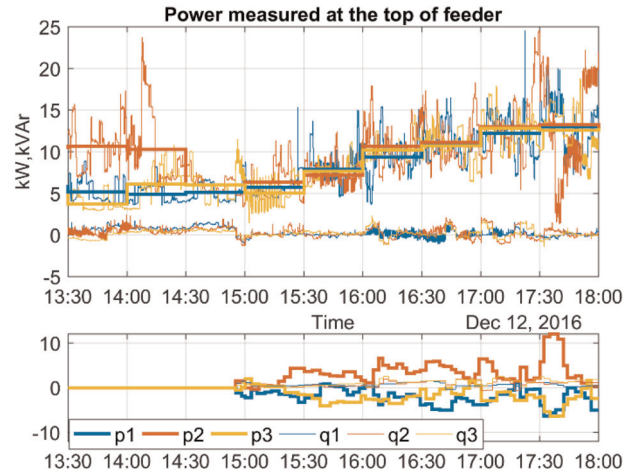


Fig. 11 Top – kW (5 s and half-hourly averages) and kVAR profiles measured at top of feeder; bottom – ESMU kW and kVAR instructions per phase

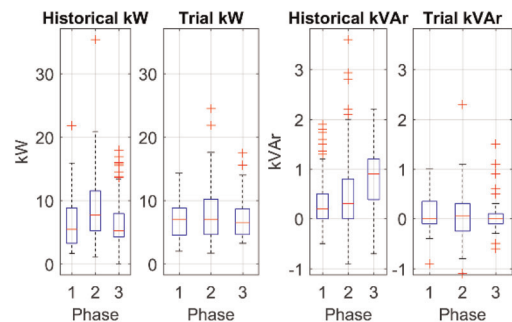


Fig. 12 Box plots of half-hourly kW and kVAR per phase from phase-balancing trial and historical data

4.3 Phase-balancing field trials

Phase-balancing and PF correction trial started at 14:40 with the control window for projection set to 3 min. Shortly after the start of the trial, the impact of ESMU operation is seen in Fig. 11: at half-hourly level, the kW loading between phases is noticeably more balanced. However, at the 5 s, the demand variation and balance between phases is high due to relatively long (3 min) control window. Fig. 12 shows the improvement on half-hourly balance between phases and reducing half-hourly reactive power, moving the average PF closer to unity.

4.4 Voltage support

To test the performance of the voltage support algorithms, the target voltage, V^t , has been set to 237 V (at 11:50) below the previous constant variation around 240 V, followed by a further step down to 235 V (at 13:10) – as depicted in Fig. 13. In response, ESMU started to increment absorption of kVAR on Phases 1 and 3. Owing to communications fault, the internal system disconnected ESMU from the network shortly before 12:30. During the ESMU outage period, voltages on Phases 1 and 3 rose back to nearly 240 V. Shortly after a further decrease in target voltage, the AIMD algorithm started to increase the absorption of kW, while maintaining a total kVA below its maximum rating by reducing the kVAR instructions.

5 Discussion

Results for phase-balancing and PF correction have shown that ESMU is capable of achieving significant improvements on

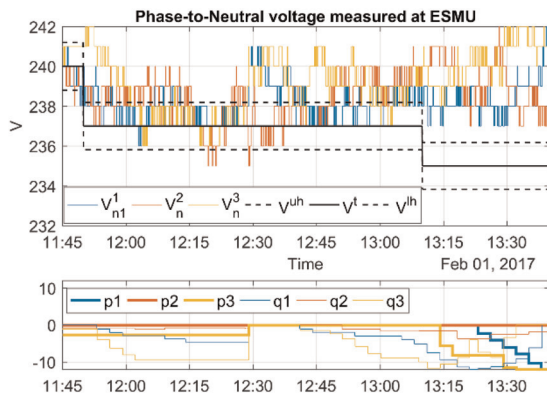


Fig. 13 (Top) Profile of phase-to-neutral voltages measured at the ESMU during the trial, with overlaid target voltage and hysteresis band. (Bottom) ESMU kW and kVAr instructions during trial

thermal constraints and line utilisation for the simulated network, while increasing the average PF. Trial results have confirmed the effectiveness of the algorithm based on comparison with historical data. However, due to differences between the actual variability in demand and duration of the control instructions, loadings between phases showed no perfect balancing. Furthermore, the assumed 0.95 PF for loads in simulation does not correspond to the reactive power demand measured before and during the trial on the real LV feeder. Simulation results of the AIMD voltage support demonstrated the effectiveness of the algorithm to adjust the kW and KVar instructions in response to change in phase-to-neutral voltage. These results also showed that the algorithm has alleviated all voltage violations compared with the baseline and improved worst phase-to-neutral voltage deviation. Trial results also demonstrated the validity of the algorithm by reducing the target voltage below the typical range. Both simulation and trial results showed that the response and effectiveness of the algorithm

is limited by the rating of the ESMU and also depend on the impedance to source.

6 Summary

The paper presented two online control algorithms designed to improve LV network operation (thermal and voltage constraints) by giving kW and kVAr instructions to a three-phase power electronics and ESU deploy on an LV feeder. Comparison of simulation and trial results has confirmed the expected effectiveness of the algorithms. Future work will include extensive analysis of the trial results and integration of the prediction mechanism to improve demand estimation.

7 Acknowledgments

This research work was carried out as part of New Thames Valley Vision (SSET203), a Low Carbon Network Fund project, funded by Ofgem and led by Scottish and Southern Electricity Networks.

8 References

- 1 Evans, G.: 'New Thames valley vision technical impact evaluation impact on DNO network from low carbon promotions', SDRC 9.8b (SSET203), 2016
- 2 Scottish and Southern Energy Power Distribution: 'Discussion document: energy storage and power electronics on the low voltage distribution network (SDRC 9.4a)', 2011. Retrieved from <http://www.thamesvalleyvision.co.uk/projectlibrary/published-documents/sdrc/manage/>
- 3 Yunusov, T., Frame, D., Holderbaum, W., *et al.*: 'The impact of location and type on the performance of low-voltage network connected battery energy storage systems', *Appl. Energy*, 2016, **165**, pp. 202–213
- 4 Zangs, M. J., Adams, P. B. E., Yunusov, T., *et al.*: 'Distributed energy storage control for dynamic load impact mitigation', *Energies*, 2016, **9**, (8), pp. 647–667
- 5 McKenna, E., Thomson, M.: 'High-resolution stochastic integrated thermal-electrical domestic demand model', *Appl. Energy*, 2016, **165**, p. 445, doi: 10.1016/j.apenergy.2015.12.089